Electronic Supplementary Material (ESI) for Nanoscale.

Supplementary Information

Visible Light-Induced Ag Nanoparticles Deposited Urchin-like Structures for Enhanced SERS Application

Rahul Purbia, Prem Depan Nayak, and Santanu Paria*

Interfaces and Nanomaterials Laboratory, Department of Chemical Engineering, National Institute of Technology, Rourkela, India

*To whom correspondence should be addressed. E–mail: sparia@nitrkl.ac.in or santanuparia@yahoo.com, Fax: +91 661 246 2999

Table of content

1. Experimental section

1.1 Materials

All the reagents of AR grade were used without any further purification. Silver nitrate (Rankem, 99.9%), trisodium citrate (Merck, 99%), sodium borohydride (Merck, 99%), polyvinylpyrrolidone (PVP, average M_W = 40,000, Sigma-Aldrich) and ultrapure water of 18.2 MΩ.cm resistivity (Millipore) were used throughout the experiments.

1.2 Characterization

The phases, structure, and crystallinity of nanostructures were obtained using an powder X-ray diffractometer (Rigaku, Japan/Ultima-IV) with Cu Kα radiation (1.5406 Å) operating at 40 kV and 30 mA. The morphologies, structures, elemental compositions, and dimensions of the nanostructures were analyzed by the scanning electron microscope (JEOL), field-emission scanning electron microscope (FEI, NOVA NanoSEM NPE212) and transmission electron microscope (FEI, Technai G20 F30). The optical property of the material was evaluated using UV-Vis-NIR spectrophotometer (Shimadzu-3600). Fourier transform infrared (FT-IR) spectroscopic characterization was carried out using a FT-IR spectrometer (Thermo Fisher, Nicolet, iS-10). The Raman spectroscopy was performed using a Triple Raman spectrometer (Horiba, T64000) equipped with 1800 grooves/mm gratings, and Ar^+ ion using 532 nm laser excitation.

1.3 Synthesis of Ag deposited urchin-like structure

Initially, Ag seed nanoparticles were prepared in aqueous solution. In this process, aqueous solution of trisodium citrate (0.3 mM) was added to $AgNO_3$ (0.1 mM) followed by addition of PVP (0.30 ml, 4 wt %) and then freshly prepared ice-cold $NaBH_4$ (0.25 mM) solution was added

drop by drop in a 10 mL working volume. The color of the suspension was changed to light yellow after seed formation. The suspension was kept under constant stirring in dark conditions for 5 min. Further, the synthesized Ag seed suspension was kept under green LED light exposure for 8 h. The final suspension color was changed to dark blue. Finally, a small amount of $AgNO_3$ (0.75 mM) was added in above-synthesized dark blue color suspension in a 2 mL vial and again exposed to green light. After 4 h exposure time, the resulting brown color suspension was centrifuged 3 times with water and ethanol to remove the impurities.

1.4 SERS application

Rhodamine 6G (R6G) dye was used as a probe to investigate the SERS detection response of the Ag deposited urchin-like substrate. After centrifugation, the collected Ag urchin-like structure were dispersed in isopropanol. Then, a small droplet of centrifuged Ag urchin-like structure colloidal suspension in isopropanol was placed on a cleaned glass surface (1 ×1 cm^2). Further, the substrate was dried for 20 min at room tempaerature, and a small drop of R6G (200 µl of 10^{-3} M) was placed onto the dried substrate. For control, same concentration and volume of R6G drop was placed onto the glass substrate. The SERS analysis was done by taking the signals from 5 randomly selected positions on the substrate using a 1 mW laser source of 532 nm wavelength. The laser beam was focused through a standard (50x) microscope objective with 0.75 numerical aperture. Each spectrum was measured once 5 second integration time with 4 number of accumulation. Thirty points on the substrate were manually assessed to examine the uniformity, which is an essential parameter for reproducible SERS measurements.

2. TEM images of Ag/PVP clusters

Figure S1 shows the FE-SEM, TEM and HADAAF-STEM images of Ag/PVP clusters. During the exposure of light, the conversion of seeds into larger size spherical NPs clusters occurs through a series of Ag redox cycles. During oxidative dissolution, Ag NPs produces Ag^+ in the suspension during light irradiation, which is again reduced by the citrate on the surface of Ag seed NPs and grow into larger size spherical NPs clusters.

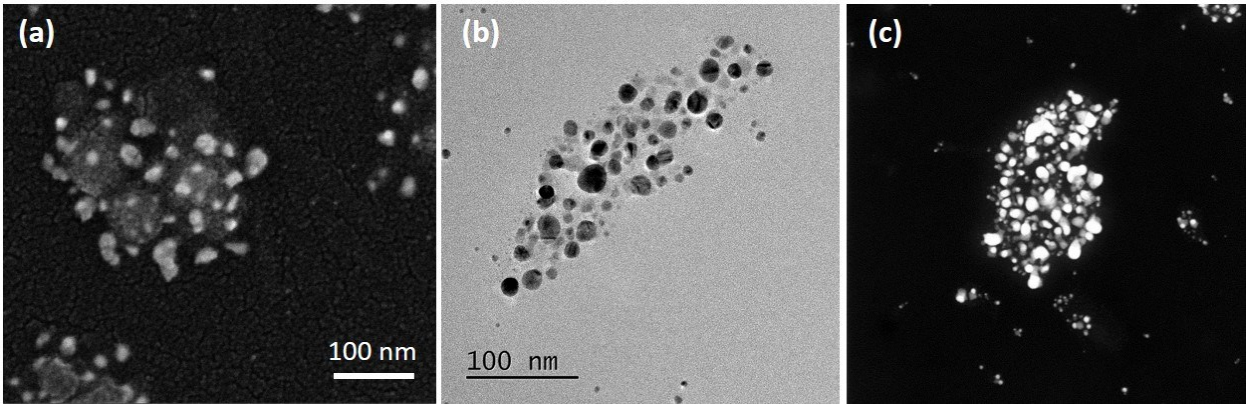

Figure S1: (a) FE-SEM, (b) TEM, (c) HADAAF-STEM images of Ag NPs clusters after 8 h green light exposure**.**

3. UV-Vis and XRD spectra of synthesized Ag NPs

Figure S2 (a) shows a UV-Vis absorption spectra and LSPR properties of synthesized Ag NPs at all three steps. Figure S2 (b) shows the XRD spectra of Ag NPs. Ag NPs were exhibited diffraction peaks (2θ) at 38.1, 44.3, 64.4, and 77.4° corresponding to the (111), (200), (220), (311) lattice planes of face-centered cubic (fcc) structure of metallic silver, respectively (JCPDS no. 04-0783).

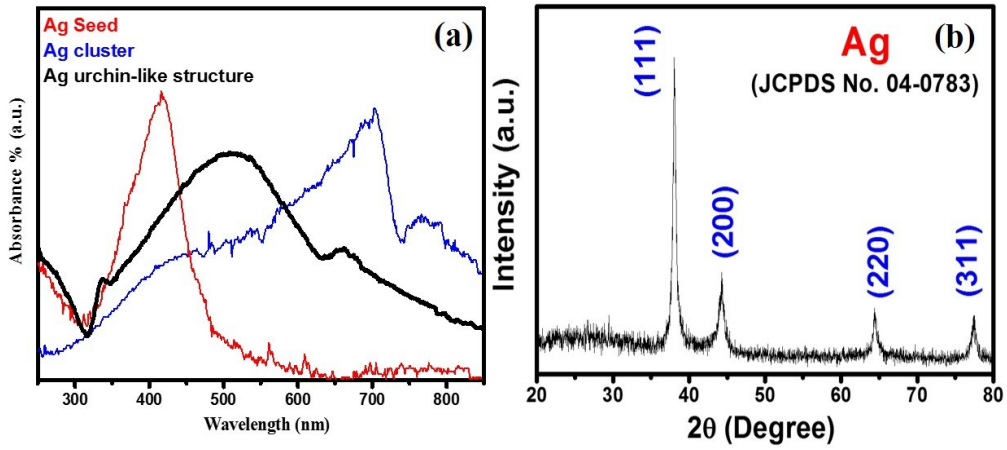

Figure S2 (a) UV-Vis spectra of Ag NPs at different stages, (b) XRD spectra of Ag urchin-like structure.

4. TEM images of the branch and center part of urchin-like Ag nanostructures

The bright-field TEM images show successful deposition of Ag NPs on the throughout surface (branch and center part) of urchin-like structures with high yield as can be seen in **Figure S3**. The average size of deposited Ag NPs were found to be 5 ±2 nm with well distributed nano-gaps between closely packed Ag NPs.

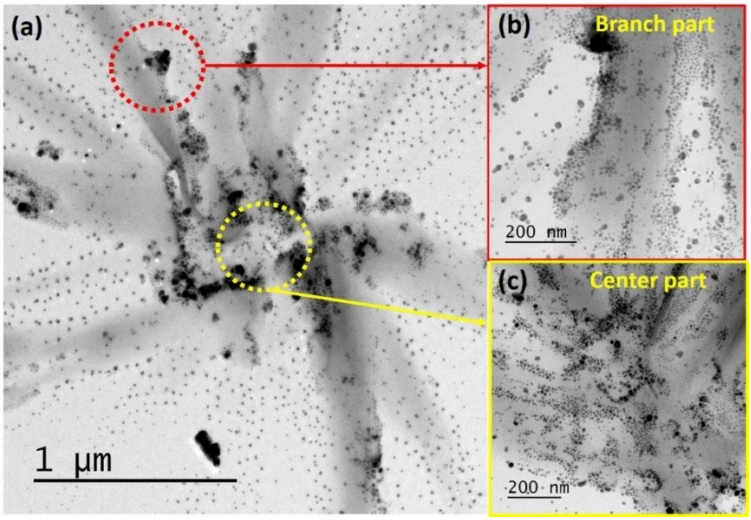

Figure S3: (a) The TEM images of urchin-like Ag nanostructure, (b) magnified view of the branch, (c) magnified view of the center part.

5. SAED pattern of as-synthesized Ag NPs on the urchin-like structure

Selected-area electron diffraction (SAED) confirmed the characteristic crystal nature of elemental silver, as clearly seen in Figure S4.

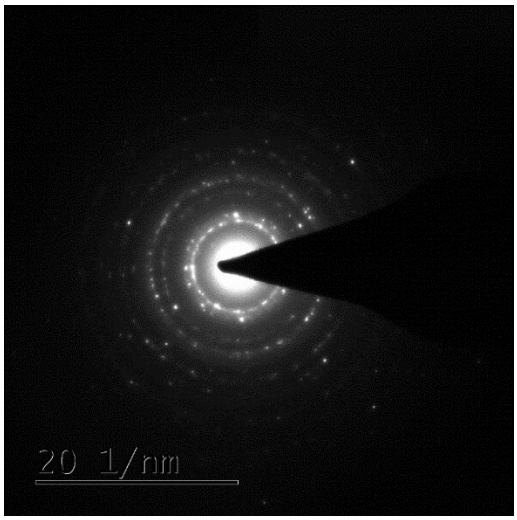

Figure S4: the continuous concentric ring-like pattern of the selected area electron diffraction pattern (SAED) of Ag NPs on the urchin-like structure.

6. Control experiments were done in the absence of PVP

Figure S5 shows the control experiments in the absence of PVP, and it was found that only Ag NPs with sized 90 ±5 were formed without PVP.

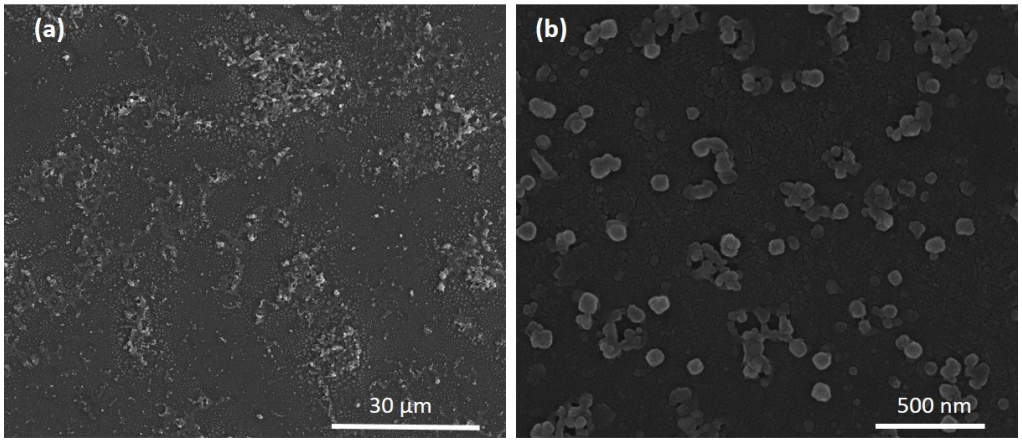

Figure S5: The control experiments were done in the absence of PVP, and it was found in FE-SEM images (a-b) that only Ag nanoparticles with sized 90 ±5 nm were formed.

7. Control experiment in the presence of $AgNO_3$ and PVP mixture

Figure S6 show the effect of Ag seeds on the final structure. The mixture of $AgNO_3$ and PVP (without seeds) were exposed to green light for 8 h and characterized using SEM and TEM. As seen in Figure, only the urchin-like fibrous polymeric structures are formed which is not similar to the urchin-like one without deposition of Ag NPs.

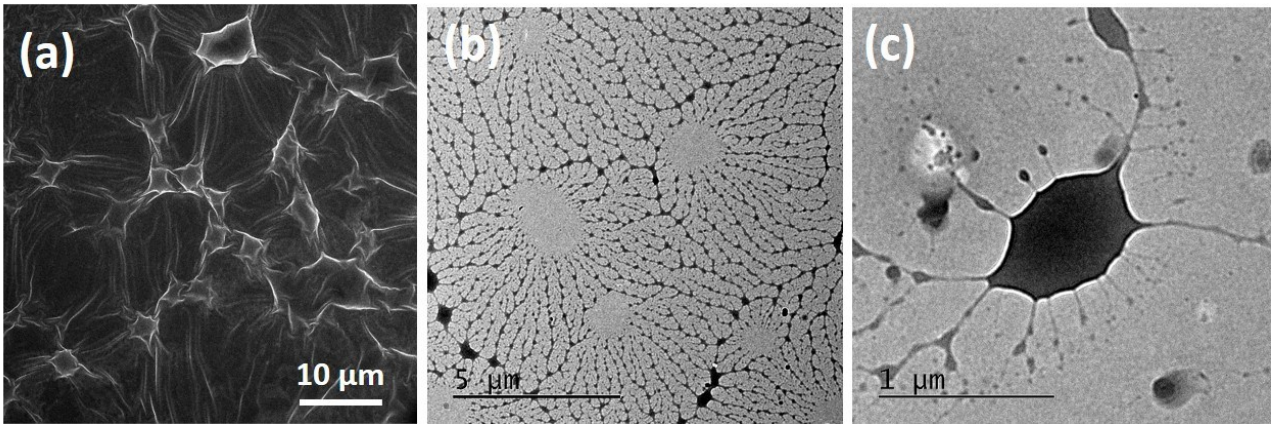

Figure S6: (a) SEM, (b-c) TEM images of the structures in the presence of $AgNO_3$ and PVP mixture indicate the formation of urchin-like coordination polymer without Ag NPs.

8. IR-spectra of as-synthesized NPs and formation mechanism

Figure S7 shows the FTIR spectra of as-synthesized structure and pure PVP. It was found that all stretching vibration peaks corresponding to the pure PVP absolutely matched with the Ag-PVP structure apart from the vibrational peak of carbonyl functional group (-C=O). The stretching vibration peak -C=O of the Ag-PVP structure (1636 cm^{-1}) was shifted to 4 cm^{-1} lower wavenumber to that of pure PVP (1640 cm^{-1}), which may be because of coordination formation.

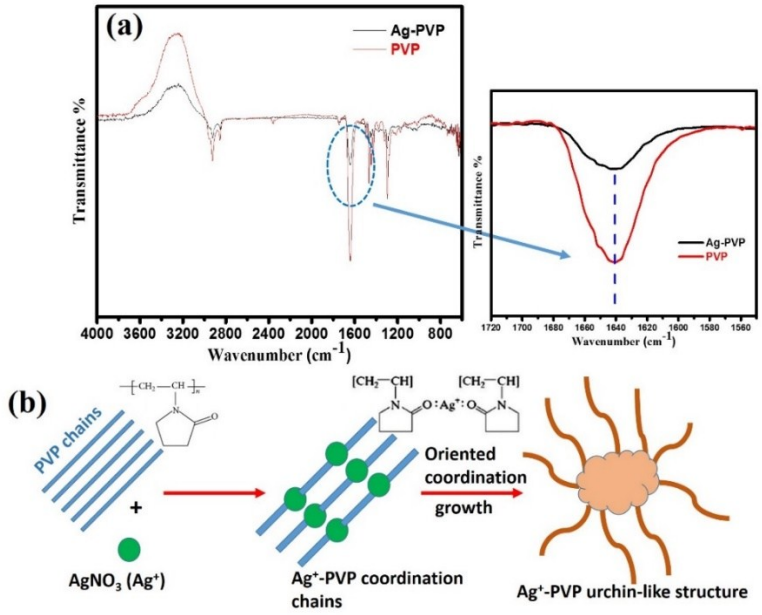

Figure S7: (a) IR-spectra of pure PVP and $AgNO_3$-PVP mixture (Ag (I)-PVP coordination polymer), left image shows magnified FT-IR stretching vibration peak -C=O, (b) schematic mechanism for the formation of Ag deposited PVP urchin-like structure.

9. SEM images of Ag urchin-like morphology with different $AgNO_3$ concentration

Figure S8 shows that the shape of urchin-like structure is highly dependent on the $AgNO_3$ concentration (effects of the $AgNO_3$ concentration on the urchin-like structures).

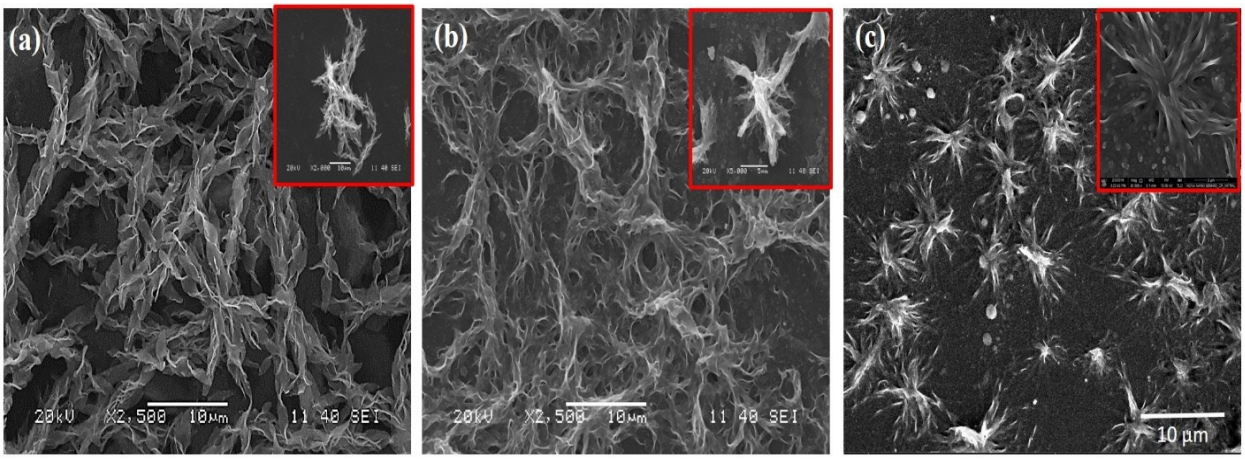

Figure S8: The SEM images of Ag fibrous morphology with different $AgNO_3$ concentration (a) 0.25 mM, (b) 0.5 mM, (c) 0.75 mM of $AgNO_3$ in the synthesized Ag seed NPs (0.1 mM).

10. Nanogaps between the formed nanoparticles on the urchin-like nanostructure

The EM field intensity can be enhanced when the nano-gap (gap in the range of subwavelength scale, i.e., below 30 nm) between two particles decreases, which in turn enhances the SERS intensity. As shown in **Figure S9**, the assembled Ag NPs into the urchin-like nanostructures have many nano-gaps (~0.8 to ~2.5 nm) between the Ag NPs.

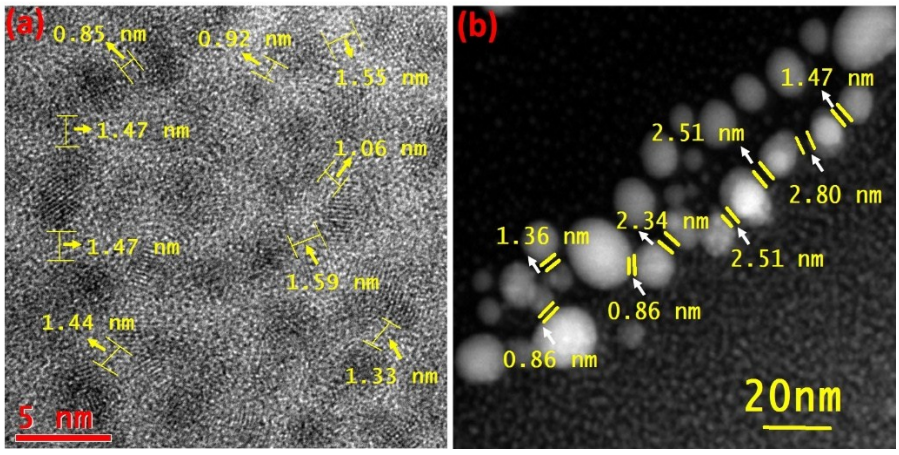

Figure S9: (a) HR-TEM and (b) HADAAF-STEM images show the nanogaps between the deposited nanoparticles on the urchin-like Ag nanostructures**.**

11. Limit of detection (LOD)

From the Raman observation, a linear standard calibration curve was obtained between Raman intensity and different concentration of R6G dye (log (M)) with correlation coefficient of > 0.99.

From the slope of linear curve, the approximately limit of detection (LOD) was found to be 10^{-12} M.

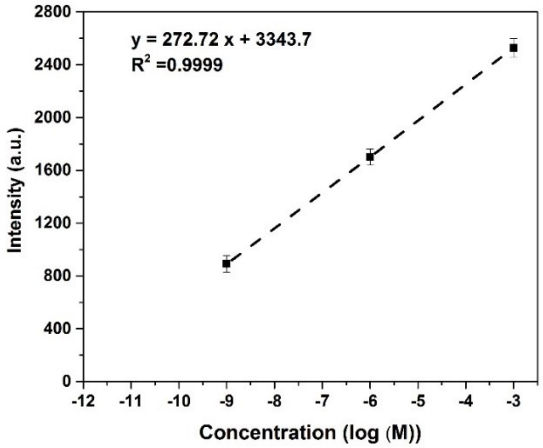

Figure S10: the linear decrease in the Raman intensity with the decrease in R6G dye concentration.

12. Cluster formation with nano-gaps on the urchin-like Ag Nanostructure

Aggregated cluster has an important role for SERS enhancement at nano-particle junctions. Figure S11 shows the representative HADAAF-STEM images of Ag NPs clusters on the urchin-like Ag nanostructure.

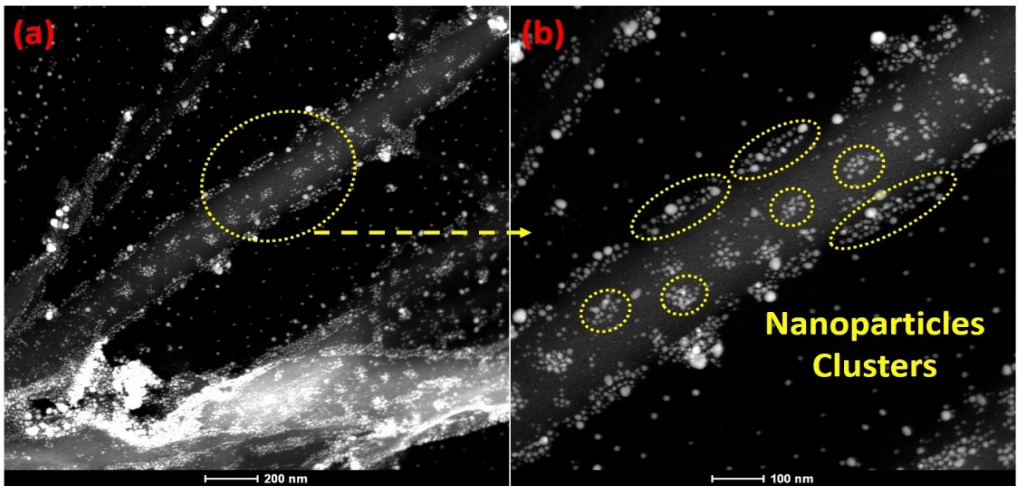

Figure S11: (a-b) representative HADAAF-STEM images showing Ag NPs clusters on the urchin-like Ag nanostructure

13. Calculation of the SERS enhancement factor (EF)

SERS EF calculation is

$$\mathbf{EF = (}I_{SERS}/I_{NR})(N_{NR}/N_{SERS})$$

where I_{SERS} and I_{NR} correspond to the integrated Raman intensities at a characteristic vibrational wavenumber of R6G molecule obtained by SERS and normal Raman scattering measurements, respectively. N_{SERS} and N_{NR} are the number of molecules probed in the SERS and normal Raman scattering measurements, respectively. I_{SERS} and I_{NR} were determined 2528, and 168 cps from the 613 cm^{-1} band, respectively, for the 10^{-3} M concentration of R6G molecule. N_{NR} was calculated through multiplying molecules concentration by the scattering volume (V) for the normal Raman (non-SERS) measurement (1.9×10^{9}). N_{SERS} value was determined by calculating the total surface area of Ag NPs (4 nm diameter) in a circular area (A) of laser spot (30 μm), assuming a spherical arrangement of R6G molecules on the particle surface (0.34×10^{2}). Here the plane area of R6G molecule is approximately assumed to be 1 nm^2 on the basis of previous reports. The EF is calculated to be 8.4×10^{8} for the 10^{-3} M R6G as the analyte.

We have considered the monolayer adsorption of R6G molecules (for highest dye concentration used, 10^{-3} M) on the surface of Ag-NPs/PVP nanostructures as per the following calculation. We consider the average size of Ag NPs is 4 nm. The particle volume and area are 32 nm^3 and 12.56 nm^2 respectively. The volume of one Ag molecule is $\frac{4}{3}\pi(0.16)^3$ = 0.017 nm^3. So, the number of molecule per particle is $\frac{R^3}{r^3} = \frac{2^3}{0.16^3}$ = 1953. Total amount of $AgNO_3$ used per SERS sample is 30

mL of 0.75 mM (concentration of $AgNO_3$ used for the synthesis of Ag NPs). So, total number of Ag molecules used was $0.75 \times 10^{-3} \times 0.03 \times 6.023 \times 10^{23}$. Total number of Ag particles formed was $\frac{0.75 \times 10 - 10^{-3} \times 0.03 \times 6.023 \times 10^{23}}{1953} = 6.9 \times 10^{15}$. Total surface area of Ag NPs = $12.56 \times 6.9 \times 10^{15} = 8.67 \times 10^{16}$ nm^2. The area occupied per dye molecule is $\frac{8.67 \times 10^{16}}{18.4 \times 10^{16}} = 0.47$ nm^2. The calculated area occupied per dye molecule is found to be higher than the actual area of a dye molecule (0.4 nm^2) reported for perpendicular orientation[1]. From this, we can assume that the molecules are forming a just monolayer with close to saturation, at the same time for lower concentrations, the molecules definitely form a monolayer.

14. SERS Enhancement Factor comparison table with previous reports

Table S1 Enhancement factor comparison table

Composition	Synthesis Process	Analyte	EF
Au nanostars on polydimethylsiloxane film[2]	Drop cast process	4-mercaptobenzoic acid	10^7
Ag-core@graphene-shell@Ag-jacket nanoparticles[3]	3-step deposition process in inert atomsphere	Rhodamine 6G	10^7
Au/Cu hybrid nanostructure arrays[4]	Using porous anodic aluminium oxide (AAO) template	urea	10^7
Ag/graphene oxide nanocomposite film[5]	thermal decomposition of a metal precursor ink followed by a tape-assisted peel-off step	Crystal Violet	2.35×10^5
Flexible membranes of Ag-nanosheet-grafted polyamide-nanofibers[6]	Electrospinning	Rhodamine 6G and 4-mercaptobenzoic acid	2.2×10^7
Cactus-like Ag Dendrites/Si Nanoneedles[7]	plasma enhanced chemical vapor deposition	Crystal Violet	6.6×10^7
Ag nanoislands on silica spheres[8]	Spray gun and thermally deposited process	Rhodamine 6G	3.76×10^7
Ag NPs on silica nanowire[9]	Reduction method on pre-synthesized silica nanowire	4-mercaptopyridine	2.9×10^8
Ag Nanostructures[10]	Pattern growth using PDMS pre-polymer	Rhodamine 6G	1.3×10^7
Ag NPs Deposited Urchin-like Structures	Visible light-induced	Rhodamine 6G	8.4×10^8

References

1 R. Sasai, T. Fujita, N. Iyi, H. Itoh and K. Takagi, *Langmuir*, 2002, **18**, 6578–6583.

2 B. Fortuni, Y. Fujita, M. Ricci, T. Inose, R. Aubert, G. Lu, J. A. Hutchison, J. Hofkens, L. Latterini and H. Uji-i, *Chem. Commun.*, 2017, **53**, 5121–5124.

3 H. Qiu, M. Wang, Z. Yang, S. Jiang, Y. Liu, L. Li, M. Cao and J. Li, *Chem. Commun.*, 2017, **53**, 8691–8694.

4 K. Chen, X. Zhang and D. R. MacFarlane, *Chem. Commun.*, 2017, **53**, 7949–7952.

5 Y. Choi, S. W. Song, W. Hooch Antink, H. M. Kim and Y. Piao, *Chem. Commun.*, 2017, **53**, 10108–10111.

6 Y. Qian, G. Meng, Q. Huang, C. Zhu, Z. Huang, K. Sun and B. Chen, *Nanoscale*, 2014, **6**, 4781-4788.

7 J. Huang, D. Ma, F. Chen, M. Bai, K. Xu and Y. Zhao, *Anal. Chem.*, 2015, **87**, 10527–10534.

8 Z. Wang, L. Feng, D. Xiao, N. Li, Y. Li, D. Cao, Z. Shi, Z. Cui and N. Lu, *Nanoscale*, 2017, **9**, 16749–16754.

9 Y. Liu, C. Deng, D. Yi, X. Wang, Y. Tang and Y. Wang, *Nanoscale*, 2017, **9**, 15901–15910.

10 M. Sakir, S. Pekdemir, A. Karatay, B. Küçüköz, H. H. Ipekci, A. Elmali, G. Demirel and

M. S. Onses, *ACS Appl. Mater. Interfaces*, 2017, **9**, 39795–39803.